

# 1 Cyclodextrin polymers as efficient adsorbents for removing toxic non- 2 biodegradable pimavanserin from pharmaceutical wastewaters

3 K. Hemine<sup>a</sup>, A. Skwierawska,<sup>a,\*</sup> A. Kernstein<sup>a</sup>, K. Kozłowska-Tylingo<sup>b</sup>

4 <sup>a</sup> Department of Chemistry and Technology of Functional Materials, Gdansk University of  
5 Technology, Narutowicza 11/12, 80-233 Gdansk, Poland

6 <sup>b</sup> Department of Pharmaceutical Technology and Biochemistry, Gdansk University of  
7 Technology, Narutowicza 11/12, 80-233 Gdansk, Poland

8 \* Corresponding author. Tel +58 347 22 88

9 *E-mail address:* [anna.skwierawska@pg.edu.pl](mailto:anna.skwierawska@pg.edu.pl) (A. Skwierawska)

10

## 11 ABSTRACT

12 Presence of even small amount of active pharmaceutical ingredients in the environment carries risks to  
13 human and animal health, presenting an important issue. The paper presents issues related to the new  
14 drug - pimavanserin (PMV). Biological treatment efficiency of pimavanserin (PMV) was evaluated  
15 using lab-scale Sequencing Batch Reactor (SBR). It has been shown to have a negative effect on aquatic  
16 organisms by classifying it as a toxic compound ( $EC_{50} = 8 \text{ mgL}^{-1}$ ). The level of biological degradation  
17 of PMV was insufficient (37%) and intensively foam formation caused operational problems. For this  
18 reason, in this study polymers based on cyclodextrins (CDs) were synthesized and used as adsorbents  
19 alternative to active carbons to effectively separate PMV from real industrial waste streams. Crosslinked  
20  $\beta$ - and  $\gamma$ -CD polymers ( $\beta$ - and  $\gamma$ -NS), obtained in reaction with carbonyldiimidazol (CDI), were fully  
21 characterized by physicochemical methods. The adsorption equilibrium data were interpreted using  
22 Freundlich and Langmuir models. The sorption process was fast (60 s) and the efficiency of PMV  
23 separation from model waste waters was 93% and 81% for  $\beta$ - and  $\gamma$ -NS, respectively. Maximum  
24 polymer capacity was found at  $52.08 \text{ mg g}^{-1}$  for  $\beta$ -NS and  $23.26 \text{ mg g}^{-1}$  for  $\gamma$ -NS. The interactions of  
25 PMV with CDs have been studied and indicate that major mechanism of the sorption is based on  
26 supramolecular interaction and capture to polymer network. Described biodegradable and reusable

27 materials are perfect example of correctly selected adsorbent for separation of target substance from  
28 postproduction aqueous media.

29

30

31 **Keywords:** cyclodextrin, polymer, pimavanserin, pharmaceutical wastewaters

## 32 **1. Introduction**

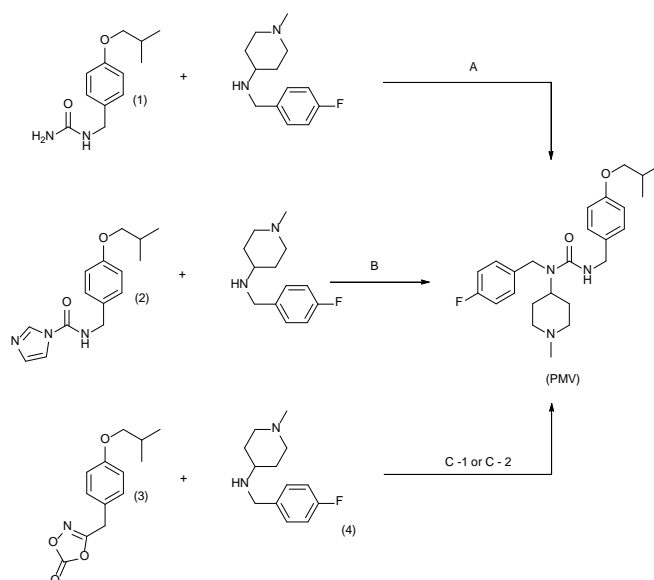
33 Wastewater from industrial and municipal streams contain undesirable organic pollutants  
34 (Morin-Crini et al., 2018). Conventional wastewater treatment technologies are not sufficient  
35 for certain pollutants removal to the desired levels (Mamba et al., 2007). The residuals of active  
36 pharmaceutical ingredients (APIs) threat the environment, human and animal health (Walter  
37 and Mitkidis, 2018). Biological (Zupanc et al., 2013), membrane processes (Shojaee Nasirabadi  
38 et al., 2016), electrochemical and chemical techniques (Ensano et al., 2017; Menapace et al.,  
39 2008), with particular emphasis on advanced oxidation (Kanakaraju et al., 2018) and adsorption  
40 processes (Al-Asheh et al., 2003; Bo et al., 2016) are the best-known industrial methods of  
41 wastewater treatment. Due to the fact that industrial effluents are very complex and time-  
42 dependent mixtures of organic and inorganic pollutants, the treatment is based on the  
43 combination of various processes that allow obtaining the required water quality in the most  
44 economical way (Morin-Crini and Crini, 2013). Of all the proposed treatments, the adsorption  
45 process is one of the most popular methods due to its simplicity, cost-effectiveness and wide  
46 range of pollutants removal from aqueous solutions.(Putra et al., 2009). Active carbons are the  
47 most common sorbents used to lower the concentration of many organic compounds in water,  
48 but the significant problem is adsorbents regeneration (Kovalova et al., 2013; San Miguel et al.,  
49 2001). Recently, much effort has been assigned to the development of cheaper and more  
50 effective adsorbents including natural polymers (Corsi et al., 2018). Oligosaccharides, such as  
51 cyclodextrins (CDs) (Arora and Dhingra, 2018; Fourmentin et al., 2018) are well known,

52 biodegradable and renewable resources (Janarthanan et al., 2016; Orprecio and Evans, 2003).  
53 Converting CDs into crosslinked polymers (nanosponges (NSs)) by condensation with bi- or  
54 multifunctional electrophilic reagents (Karoyo and Wilson, 2016; Pratt et al., 2010; Szejtli et  
55 al., 1978) allows to obtain water insoluble natural adsorbents used in separation and purification  
56 processes (Morin-Crini and Crini, 2013). The adsorption mechanism of NSs is related to  
57 inclusion complexation, physical sorption in network and hydrogen bonding (Crini et al., 1998;  
58 Yilmaz et al., 2010).

59 Many modern drugs have complex chemical structure. Pimavanserin (PMV) belongs to  
60 this category. PMV is an atypical antipsychotic drug, recommended for the treatment of  
61 hallucinations and delusions associated with Parkinson's psychosis (Chendo and Ferreira,  
62 2016). The Food and Drug Administration agency approved PMV as the first drug to treat  
63 Parkinson's disease in 2016 and it is also being developed to treat other psychotic disorders,  
64 including schizophrenia (Combs and Cox, 2017). With the increasing role in pharmaceutical  
65 treatment, the amount of PMV discharged to the environment may increase accordingly,  
66 therefore toxicity and biodegradability tests are necessary. To the best of the authors'  
67 knowledge, no such studies have been carried out.

68 Additionally, it should be emphasized that so far attention has been given to make PMV  
69 synthesis environmentally friendly. The biggest achievement is the exclusion of isocyanates  
70 and replacing them with raw materials obtained by reaction with urea and carbonic acid  
71 derivatives (Fig. 1). What important is that, the acids derivatives could be used directly in the  
72 main reaction without the need for isolation and the intermediate purification. The obtained  
73 PMV solution in an organic solvent (usually ethyl acetate) is purified by repeated extraction  
74 with water or aqueous solutions of HCl ( $\text{NH}_4\text{Cl}$ ) and NaCl. At this stage post-production  
75 raffinates containing different amount of PMV are produced.





76  
 77 **Fig. 1.** Raw materials used in the synthesis of PMV, excluding isocyanates. Waste streams generated during the  
 78 synthesis of PMV in method: A and B - aqueous raffinate, C-1 aqueous raffinate contain  $\text{NH}_4\text{Cl}$  and  $\text{NaCl}$ ; C-2  
 79 acidic raffinate contain  $\text{HCl}$  and  $\text{NaCl}$  (Chen-Wei and Chin-Wei, 2018; Rapolu et al., 2019)

80 In this work, preliminary PMV toxicity and biodegradability studies were evaluated.  
 81 We have proposed the use of water-insoluble NS based on  $\beta$ - and  $\gamma$ -CD as adsorbents for the  
 82 separation of this drug from industrial raffinates. NSs were obtained by condensation  
 83 polymerization reactions with a carbonyl cross-linked 1,1'-carbonyldiimidazole (CDI) (Trotta  
 84 and Tumiatti, 2005). The obtained NSs were characterized in detail. Studies were focused to  
 85 achieve the best conditions of adsorption. After each sorption stage, the NSs were regenerated.  
 86 Finally, the adsorption efficiency of NSs were compared with the adsorption efficiency  
 87 obtained with the use of commercially available activated carbons. The adsorption mechanisms  
 88 of PMV by NSs were investigated, based on the interaction between drug and natural  
 89 cyclodextrin. In addition to only one the patent available in the literature, which mentions that  
 90 cyclodextrins can be used in pimavanserin preparations as complexing agents (Gant and  
 91 Sarshar, 2008), detailed study on interaction of PMV with CDs has not been published so far.  
 92 This work offers a new way to effectively separate pollutants from wastewater by using  
 93 selective, biodegradable and fully regenerable materials based on cyclic oligosaccharides. The



94 presented research concerns the area of environmentally friendly technologies and can be easily  
95 accessible to large-scale fabrication.

## 96 97 **2. Materials and methods**

### 98 2.1. Chemicals and materials

99 Pimavanserin tartrate (PMV,  $\geq 99.9\%$ ) and free base (PMV-b) was synthesized, based  
100 on procedures described in patent US2018/0208556 A1(Chen-Wei and Chin-Wei, 2018).  
101 Pimavanserin tartrate standard was obtained from LGM Pharma (USA). 1,1'-  
102 carbonyldiimidazol (CDI,  $\geq 98\%$ ), methanesulfonic acid ( $\text{CH}_3\text{SO}_3\text{H}$ ,  $\geq 99\%$ ),  $\beta$ -cyclodextrin  
103 ( $\beta$ -CD,  $\geq 97\%$ ) and  $\gamma$ -cyclodextrin ( $\gamma$ -CD,  $\geq 98\%$ ) were purchased from Sigma-Aldrich.  
104 Acetonitrile (HPLC-grade) was supplied by Chempur (Poland). Methanol ( $\text{CH}_3\text{OH}$ ,  $\geq 99.8\%$ ),  
105 ethanol ( $\text{C}_2\text{H}_5\text{OH}$ , anhydrous,  $\geq 99.8\%$ ), and dimethyl sulfoxide ( $(\text{CH}_3)_2\text{SO}$ ,  $\geq 99.9$ ) were  
106 purchased from POCH. Potassium bromide (KBr, spectroscopy grade) were purchased from  
107 Fisher Scientific and dried before use. All chemical were used without further purification.  
108 Water used in all experiments was purified by Hydrolab-system (HLP- SPRING, temp. 22 °C,  
109  $\kappa = 2.70 \mu\text{S}$ ). Activated carbons Norit SX1 ( $S_{\text{BET}} = 900 \text{ m}^2/\text{g}$ ) (N-SX1) was obtained from  
110 Brenntag and Organosorb 200-C303 ( $S_{\text{BET}} = 1200 \text{ m}^2/\text{g}$ ) (O-C303) was obtained from Lenntech.

### 112 2.2. Synthesis procedures

113  $\beta$ - and  $\gamma$ -NS were synthesized following the procedure previously reported (Trotta and Tumiatti,  
114 2005) with some minor modifications. Detailed information on the synthesis of NSs, their  
115 analysis, as well model post-production raffinates preparation are presented in SI (Text S3 and  
116 S4, Fig. S1-S8, Table S1-S5).

117



### 118 2.3. Methods

119 Biological experiments were performed using the activated sludge donated from  
120 municipal wastewater treatment plant (Swarzewo, Poland). The biological unit of this treatment  
121 plant was sequencing batch reactor (SBR). The total suspended solids of the sludge samples  
122 were determined according to standard methods reported by American Public Health  
123 Association (American Public Health Association (APHA), 2005).

124 The progress of PMV biological degradation was determined using high-performance  
125 liquid chromatography (HPLC). Toxicity test of PMV was performed by the Microtox bioassay  
126 according to the Strategic Diagnostic (USA) company's standard procedure requirements  
127 (details in SI, Text S1, S2).

128 Adsorption experiments of PMV were studied at 25°C using digital vortex mixer  
129 (OHAUS VXHDDG) at 1,000 rpm. Aqueous suspension used for PMV removal experiments  
130 were centrifuged at 11,000 rpm for 10 min (MPW-250) and filtered through glass microfiber  
131 filters (Whatman, grade GF/F).

132 Ultraviolet-visible (UV-vis) spectra were recorded over the range 190-400 nm (HACH  
133 LANGE UV-VIS DR 6000), corrected against appropriate background spectrum.

134 Infrared spectroscopy (FT-IR) was performed on a Thermo Nicolet iS10 using the KBr  
135 pellet method. The spectral resolution was 4 cm<sup>-1</sup> and the scanning range was from 400 to 4000  
136 cm<sup>-1</sup>.

137 The Nuclear Magnetic Resonance (NMR) spectra were recorded in D<sub>2</sub>O on a Bruker  
138 Avance III HD 400 MHz spectrometer at 25 °C.

139 Nitrogen (N<sub>2</sub>) adsorption-desorption isotherms were conducted at 77 K using ASAP  
140 2420 V2.09A apparatus. The specific surface area was measured by the Brunauer-Emmett-  
141 Teller (BET) (Brunauer et al., 1938) method and pore size distribution (PSD) was measured

142 using the classical Barrett-Joyner-Halenda (BJH) model (Barrett et al., 1951) and the Harkins  
143 and Jura t-Plot method.

144 Scanning electron micrograph (SEM) observation was performed on a Quanta FEG 250  
145 scanning electron microscope.

#### 146 2.4. Biological treatment

147 The PMV biological treatment was performed in a special model reactor with a working  
148 volume of 5 L. The reactor was equipped with an aeration system O<sub>2</sub>, stirrer, pH and  
149 temperature sensors. The activated sludge was aerobically conditioned for 24 hours to minimize  
150 pollutants level. Then, activated sludge was mixed with PMV wastewater in concentration of  
151 10<sup>-3</sup> M. After 30 minutes the mixture was withdrawn, filtered using paper filter (00A102.180,  
152 Chemland) and the chemical oxygen demand (COD) (Vial Test, Hach), and ammonia nitrogen  
153 (Nitrogen-Ammonia reagent set, Nessler, Hach) were measured. The whole experimental  
154 process lasted 24 hours, per analogy to real purification cycle in municipal water resource  
155 recovery facility in Swarzewo. Reactors were operated under anoxic/aerobic conditions, in  
156 which the first three hours were anoxic (dissolved oxygen DO ≤ 0.1 mgO<sub>2</sub> L<sup>-1</sup>) followed by  
157 aeration (DO 2.5-5 mg O<sub>2</sub> L<sup>-1</sup>). After 24 hours a sample was taken again, treated as above and  
158 analyzed. To determine the total PMV removal after 24 hours of biological wastewater  
159 treatment, the possible residual drug was also analyzed on the activated sludge. For this purpose,  
160 the precipitate was filtered, frozen at -20 °C, and then lyophilized in a freeze-dryer (Novalyphe-  
161 NL 500) for 24 h at -50 °C. The resulting brown powder was homogenized by grinding, then  
162 extracted with methanol and the drug content determined using HPLC.

163 The percentage removed of PMV during biological wastewater treatment process was  
164 calculated according to the equation:

$$165 \text{ Removal efficiency (\%)} = \frac{D_{0(\text{min})} - (D_{24(\text{hours})} + D_{AS})}{D_{0(\text{min})}} \cdot 100$$



166 where  $D_{0(\min)}$  (g) is the initial content of PMV,  $D_{24(\text{hours})}$  (g) and  $D_{AS}$  (g) are the PMV content in  
167 filtrate and active sludge after 24 hours of biological wastewater treatment process,  
168 respectively.

## 169 2.5. Adsorption experiments

170 All experiments were carried out at ambient temperature using PMV aqueous solution  
171 ( $85.5 \text{ mg L}^{-1}$ ). In each study, accurately weighed amount of adsorbent was transferred to 5 mL  
172 of PMV solution in plastic vials (7 mL) and sealed. The mixture was then shaken on a digital  
173 vortex mixer at 1,000 rpm. Experiments were performed for various time intervals to determine  
174 the adsorption equilibrium and maximum amount of PMV adsorbed. The solid phase was  
175 separated by centrifugation and filtration. The PMV concentrations in solutions were measured  
176 spectrometrically at  $\lambda_{\max} = 271 \text{ nm}$ . The efficiency of removal of PMV (%) by  $\beta$ -NS or  $\gamma$ -NS  
177 was calculated based on the following equation:

$$178$$
$$179 \text{ Adsorption efficiency (\%)} = \frac{C_0 - C_e}{C_0} \times 100 \quad (1)$$
$$180$$

181 where  $C_0$  ( $\text{mg L}^{-1}$ ) and  $C_e$  ( $\text{mg L}^{-1}$ ) are the initial and equilibrium concentration of PMV in the  
182 stock solution and filtrate, respectively.

183 The amount of PMV adsorbed was determined by the following equation:

$$184$$
$$185 q_e = \frac{(C_0 - C_e)V}{m} \quad (2)$$
$$186$$

187 where  $q_e$  ( $\text{mg g}^{-1}$ ) is the amount of PMV bound to the sorbent per g of sorbent,  $m$  (g) the mass  
188 of sorbent used in the experiment,  $V$  (L) the volume of PMV solution used.



189 The influence of the pH was determined at a pH ranging from 1.0 to 8.0 and adjusted with  
190 NaOH (0.01M) or HCl (0.01M)2.6. Adsorption isotherms

191 30 mg of  $\beta$ -NS or 120 mg of  $\gamma$ -NS was accurately weighed and transferred to a 7 mL  
192 plastic vials, and 5 mL of PMV stock solutions ranging from 42.8 to 428 mg L<sup>-1</sup> was added.  
193 Then, the mixtures were shaken on digital vortex mixer at 1,000 rpm for 30 min to reach  
194 equilibrium. Then, the suspensions were separated by centrifugation and filtration. The  
195 absorbance of the filtrates was measured at wavelength at  $\lambda_{\max}= 271$  nm.

196

#### 197 2.6.1. Freundlich isotherm

198 This type of isotherm is an empirical equation employed to describe an adsorption on  
199 heterogeneous surfaces and is calculated using the following equation (Rao et al., 2012):

$$200 \quad q_e = K_F C_e^{1/n_F} \quad (3)$$

201 where,  $q_e$  (mg g<sup>-1</sup>) is the equilibrium PMV concentration on adsorbent,  $C_e$  (mg L<sup>-1</sup>) is the  
202 concentration of PMV at equilibrium in solution,  $K_F$  (L g<sup>-1</sup>) is the Freundlich constant and  $1/n_F$   
203 is the heterogeneity factor.

204 A linear form of the Freundlich adsorption isotherm was obtained by plotting  $\ln q_e$  versus  
205  $\ln C_e$  in the following equation:

$$206 \quad \ln q_e = \frac{1}{n_F} \ln C_e + \ln K_F \quad (4)$$

#### 207 2.6.2. Langmuir isotherm

208 The non-linear expression of Langmuir isotherm model is represented as follows (Ho et  
209 al., 2002):



210  $q_e = \frac{x}{m} = \frac{K_L C_e}{1 + a_L C_e}$  (5)

211 where,  $q_e$  ( $\text{mg g}^{-1}$ ) is the equilibrium PMV concentration on adsorbent,  $x$  (mg) is the amount of  
212 PMV adsorbed,  $m$  (g) the amount of adsorbent used,  $C_e$  ( $\text{mg L}^{-1}$ ) is the concentration of PMV  
213 at equilibrium in solution,  $a_L$  ( $\text{L mg}^{-1}$ ) and  $K_L$  ( $\text{L g}^{-1}$ ) are the Langmuir isotherm constants.

214 Langmuir adsorption isotherm in a linear form was generated by plotting  $C_e q_e^{-1}$  against  
215  $C_e$  in the following equation:

216  $\frac{C_e}{q_e} = \frac{a_L}{K_L} C_e + \frac{1}{K_L}$  (6)

217 The maximum adsorption capacity,  $q_{\text{max}}$  of the adsorbent described the theoretical  
218 monolayer capacity was calculated as follows:

219  $q_{\text{max}} = \frac{K_L}{a_L}$  (7)

220 The equilibrium parameter,  $R_L$ , also called the separation factor, is calculated using the  
221 equation (Hall et al., 1966; McKay, 2007):

222  $R_L = \frac{1}{1 + a_L C_0}$  (8)

223 where,  $C_0$  is the initial concentration ( $\text{mg L}^{-1}$ ).

224 The  $R_L$  value assumes feasibility and the nature of adsorption process is specified in the  
225 following: irreversible ( $R_L=0$ ), favorable ( $0 < R_L < 1$ ), linear ( $R_L=1$ ), unfavorable ( $R_L > 1$ ).2.7.

226 Regeneration experiments

227 0.03 g of  $\beta$ -NS or 0.12 g of  $\gamma$ -NS was accurately weighed and transferred to a 7 mL  
228 plastic vial, and 5 mL PMV stock solution ( $0.2 \text{ mmol L}^{-1}$ ) was added. Then, the suspension was  
229 shaken on digital vortex mixer at room temperature for 30 minutes. After this time, the mixture

230 was centrifuged and filtered through Whatman glass microfiber filters (grade GF/F). The PMV  
231 content in the filtrate was determined spectrophotometrically. Material regeneration was carried  
232 out according to the developed methodology based on five times rinsing with methanol (5x 10  
233 mL), spectrophotometric checking of the presence of PMV in the last filtrate, in the case of  
234 content below the detection limit, the material was further washed five times with water (5x10  
235 mL) to remove polar substances and salts. Otherwise the procedure was repeated and the next  
236 step was to rinse with water. Finally, the adsorbents were again washed with 10 mL MeOH to  
237 remove water from the NS. Then the NS was dried to constant weight on a moisture analyzer  
238 and reused in the PMV adsorption process. This adsorption-desorption cycle was carried out  
239 three times.

## 240 2.8. Purification of model post-reaction raffinates.

241 From each sample, 5 mL of the solution was withdrawn and quantitatively transferred to  
242 falcon tube containing 75 mg  $\beta$ -NS or 25 mg of activated carbon O-C303. The content of falcon  
243 tubes was shaken, this time for 30 min due to the higher concentration of PMV and the presence  
244 of additional substances in the samples.

245 All adsorption experiments were performed in triplicate.

## 246 3. Results and discussion

### 247 3.1. Biological treatment

248 To study the biological treatment efficiency of PMV, the chemical oxygen demand  
249 (COD), ammonium ( $\text{N-NH}_4^+$ ) and drug content (DC) before and after degradation were  
250 determined. To assess the possibility of precipitation of the compound during the degradation  
251 process, the content of the drug after 30 min of aeration and its residue on the activated sludge  
252 after 24 hours were also determined. The results presented in Table 1 show, that degree of

253 removal of PMV is only 37%. An almost three-fold increase in the concentration of ammonium  
 254 nitrogen is observed and a slight increase of the COD parameter indicating the adverse effect  
 255 of PMV on the active sludge organisms. In this situation, the bacteriostatic effect of the drug  
 256 cannot be ruled out, which inhibits the nitrification and denitrification processes, consequently  
 257 the initial ammonification process proceeds with low efficiency. During the biological  
 258 treatment of PMV wastewater, significant foaming of the activated sludge is observed, which  
 259 undoubtedly causes serious problems in its operation. In addition, the standard Microtox test  
 260 showed a very low  $EC_{50}$  level for PMV ( $EC_{50} = 8 \text{ mgL}^{-1}$ ) and according to the Waste Framework  
 261 Directive (WFD, 2008/98 / EC) the drug can be classified as hazardous to the environment  
 262 (Weltens et al., 2014).

263 **Table 1.**  
 264 Composition of treated wastewater of PMV.

Parameters	Before treatment	After treatment (24 hours)
COD [ $\text{mgO}_2 \text{ L}^{-1}$ ]	362	392
N-NH <sub>4</sub> <sup>+</sup> [ $\text{mgN-NH}_4^+ \text{ L}^{-1}$ ]	0.76	2.05
DC [g]	0.151 (0 min)	0.066
	0.075 (30 min)	0.029 (AS)

265 COD- chemical oxygen demand; N-NH<sub>4</sub><sup>+</sup> ammonium; DC- content of PMV; AS- active sludge.

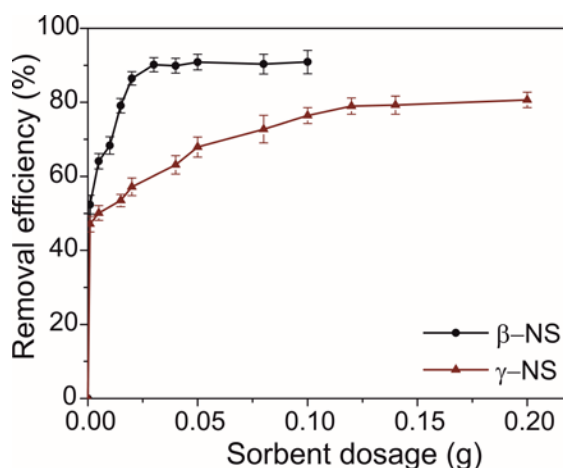
266

## 267 3.2. Adsorption experiments

### 268 3.2.1. Effect of adsorbent mass

269 The adsorption of PMV on NSs ( $\beta$ -NS or  $\gamma$ -NS) was studied by maintaining constant  
 270 volume of stock solution of PMV ( $85.5 \text{ mg L}^{-1}$ ), temperature ( $25 \text{ }^\circ\text{C}$ ) rotation speed (1,000  
 271 rpm), contact time (30 min) and pH ( $\text{pH} = 7$ ) whilst changing the amounts of sorbent in the  
 272 solution. The results presented in Fig. 2 show that the percentage of PMV removal increased  
 273 with the adsorbent dosage. The gradual increase in sorption due to the increased mass of the  
 274 adsorbent is typical and is the result of incomplete filling of the NS surface. After saturation of

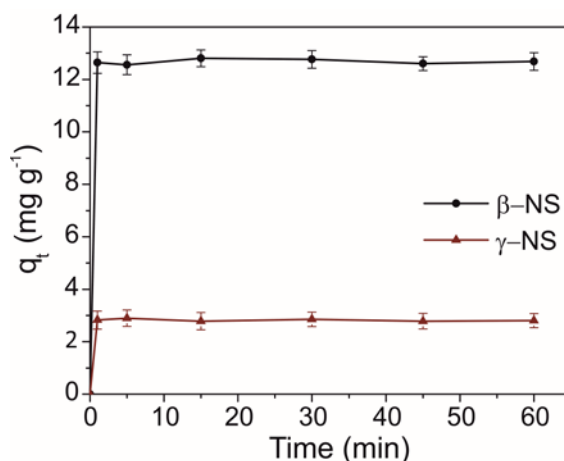
275 the material, stabilization occurs, and consequently the amount of adsorbed drug is constant.  
276 For this reason, 0.03 g ( $\beta$ -NS) and 0.12 g ( $\gamma$ -NS) mass of adsorbent were chosen for the next  
277 experiments.



278  
279 **Fig. 2.** Effect of adsorbent mass on the removal efficiency of PMV by  $\beta$ -NS (black) and  $\gamma$ -NS (red); PMV  
280 concentration = 85.5 mg L<sup>-1</sup> and solution volume 5 mL; contact time = 30 min, temperature = 25 °C, , pH = 7,  
281 rotational speed (1,000 rpm).

282  
283 3.2.2. Effect of contact time

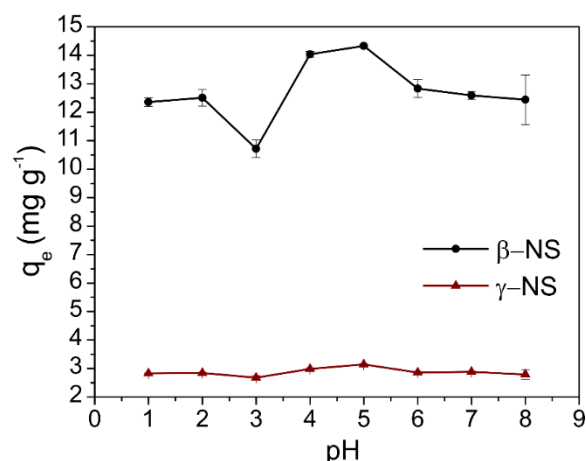
284 A series of experimental data for the adsorption of PMV versus contact time is presented  
285 in Fig. 3. All the experiments were performed at pH = 7 with initial concentration of PMV (85.5  
286 mg L<sup>-1</sup>), amount of adsorbent (0.03 g for  $\beta$ - and 0.12 g for  $\gamma$ -NS) and agitation speed (1,000  
287 rpm). It was observed that both cyclodextrin adsorbents required less than 1 min to reach  
288 equilibrium and the maximum amounts of PMV adsorbed were 12.8 and 2.9 mg g<sup>-1</sup> for  $\beta$ - and  
289  $\gamma$ -NS, respectively.



290  
 291 **Fig. 3.** Effect of time on the adsorption of PMV by  $\beta$ -NS (black) and  $\gamma$ -NS (red); PMV concentration = 85.5 mg  
 292  $\text{L}^{-1}$  and solution volume 5 mL; room temperature, pH = 7, temperature = 25 °C, rotational speed (1,000 rpm).

293  
 294 3.2.3. Effect of pH

295 It is well known that pH of the solution plays an important role during the process of pollutants  
 296 adsorption. The acidity and basicity of the solution can easily change the ionization degree of  
 297 the adsorbate. The adsorption of PMV on NSs (0.03 g for  $\beta$ - and 0.12 g for  $\gamma$ -NS) was studied  
 298 by maintaining constant volume of stock solution of PMV (85.5  $\text{mg L}^{-1}$ ), temperature (25°C),  
 299 rotation speed (1,000 rpm), contact time (30 min), whilst changing the value of pH of solution.  
 300 Fig. 4 exhibits that the PMV uptake by  $\beta$ - and  $\gamma$ -NS are slightly influenced by pH in the range  
 301 of 1-2 and 5-8. Conducting tests in the  $\text{pH} > 8$  range is not possible due to the two-phase system.  
 302 It is well known that pimavanserin in the form of the free base shows limited solubility in water  
 303 and even less in the case of an alkaline environment. The polymer material itself is not sensitive  
 304 to pH due to the lack of groups capable of ionizing in such mild conditions.



305

306 **Fig. 4.** Effect of pH on PMV adsorption capacities of  $\beta$ - and  $\gamma$ -NS.

307

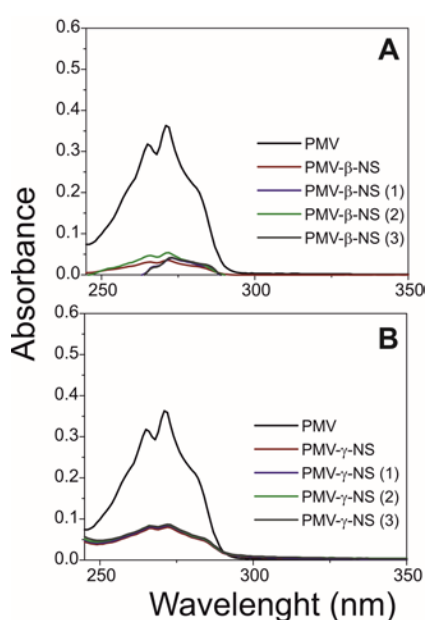
### 308 3.2.4. Effect of adsorbent type

309 The adsorption experiments were performed for the uptake of PMV through various  
 310 type of adsorbents ( $\beta$ -NS,  $\gamma$ -NS, O-C303 and N-SX1) with a constant initial drug concentration  
 311 of 85.5 mgL<sup>-1</sup>. On the first stage of experiment, we decided to select carbon adsorbents mass  
 312 for adsorption equilibrium, as it was done for  $\beta$ - and  $\gamma$ -NS (Fig. S9). Finally, the studies were  
 313 performed for the mass of 0.03 g, 0.12 g, 0.01 g and 0.02 g for  $\beta$ -NS,  $\gamma$ -NS, O-C203 and N-  
 314 SX1, respectively, and the time of 1 min. According to the results, we can conclude that all  
 315 types of adsorbents enabled PMV removal from aqueous solution with high efficiency: 92.95,  
 316 92.67, 91.82 and 80.50% for O-C303,  $\beta$ -NS, N-SX1, and  $\gamma$ -NS, respectively within  
 317 impressively short time.

### 318 3.2.5. Regeneration experiments

319 An undoubted advantage of the presented NSs is the possibility of their simple  
 320 regeneration and reuse. The important thing is that the effectiveness of PMV adsorption with  
 321 the use of regenerated materials remain at a similar level, as evidenced by the results presented  
 322 in the form of UV-vis spectra in Fig.5. The difference is small and amounts to 5.4% (87.6-

323 93.0%) and 2% (78.5-80.5), for  $\beta$ -NS and for  $\gamma$ -NS, respectively. During regeneration, multiple  
324 rinsing with water can be applied. The advantage of the method is the use of an environmentally  
325 friendly solvent. The disadvantage is the considerable volume of the waste aqueous drug  
326 solution. A much better method is the use of methanol, a very selective PMV extractant. From  
327 the resulting solution, the solvent can be easily regenerated by distillation, affording the PMV,  
328 and reused. Rinsing with methanol do not affect the structure of the material as evidenced by  
329 the FTIR spectra after each stage of the regeneration process (Fig. S8).



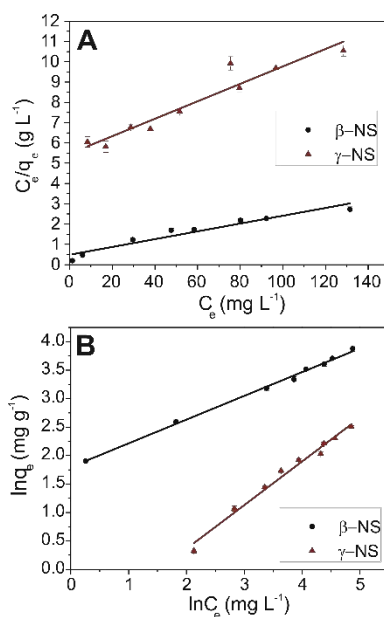
330  
331 **Fig. 5.** UV-vis spectra recorded before and after regeneration process (one to three times) for  $\beta$ -NS (A) and  $\gamma$ -NS  
332 (B).

### 333 3.2.6. Adsorption equilibrium

334 The Langmuir and the Freundlich isotherms were used to express the distribution of  
335 PMV between the adsorbent and the solution at equilibrium. Adsorption experiments were  
336 performed for different initial PMV concentrations (42-421 mg L<sup>-1</sup>), maintaining a constant pH  
337 = 7, temperature (25 °C), contact time (30 min) and agitation speed (1,000 rpm).



338 Data obtained from adsorption experiments were expressed using the Langmuir and  
339 Freundlich isotherms (Fig. 6).



340  
341 **Fig. 6.** Langmuir (A) and Freundlich (B) isotherm of PMV adsorption by  $\beta$ -NS (black) and  $\gamma$ -NS (red).

342 The results obtained show that both isotherms are linear within all established initial  
343 concentrations. The determined values including correlation coefficients ( $R^2$ ) indicate a worse  
344 adjustment to the Langmuir model ( $R^2 = 0.93$  for  $\beta$ -NS and  $R^2 = 0.92$  for  $\gamma$ -NS; Fig. 5A) than  
345 the Freundlich model ( $R^2 = 0.99$  for  $\beta$ -NS and  $R^2 = 0.98$  for  $\gamma$ -NS, Fig. 5B). Freundlich's  
346 isotherm describes sorption on heterogeneous surfaces or surfaces with different affinities. The  
347 model assumes that the stronger binding sites are first occupied and the binding force decreases  
348 with the degree of occupancy. The adsorption parameters of Freundlich and Langmuir are given  
349 in Table 2. The values of the Freundlich exponent  $n=2.40$  ( $\beta$ -NS) and  $n=1.30$  ( $\gamma$ -NS) in the  
350 range of 1-10 described favorable adsorption. For the Langmuir-model adsorption the  
351 dimensionless constant separation factor ( $R_L$ ) was calculated according to Eq. 8 to classify  
352 isotherm shape. The  $R_L$  value lying in the range of 0-1 confirms the favorable uptake of the  
353 PMV. According to the obtained results, the Freundlich isotherm is reliable model describing the  
354 PMV removal from water by NSs. This is related to heterogeneous surfaces of NSs (data are

355 presented in SI, Fig. S2-S4 and Table S3-S5). The presence of heterogeneous absorption sites  
 356 on the CD-NS surfaces is also visually confirmed based on the SEM analysis (Fig. S8).

357 **Table 2**  
 358 Parameters of the equilibrium sorption models and of linear ( $R^2$ ) regression coefficient.

Equilibrium model	Parameter	Value	
		$\beta$ -NS	$\gamma$ -NS
Langmuir isotherm	$q_{\max}$ ( $\text{mg g}^{-1}$ )	$52.08 \pm 2.59$	$23.26 \pm 1.01$
	$K_L$ ( $\text{L g}^{-1}$ )	$2.05 \pm 0.21$	$0.18 \pm 0.01$
	$a_L$ ( $\text{L mg}^{-1}$ )	$0.04 \pm 0.002$	$0.01 \pm 0.0003$
	$R_L$	0.06-0.38	0.25-0.77
	$R^2$	0.93	0.92
Freundlich isotherm	$K_F$ ( $\text{L g}^{-1}$ )	$6.03 \pm 0.17$	$0.31 \pm 0.02$
	$n_F$	$2.40 \pm 0.03$	$1.30 \pm 0.03$
	$R^2$	0.99	0.98

359  
 360 For comparison of the sorption capacity of different cyclodextrin based adsorbents, the  $q_{\max}$   
 361 parameter obtained with the Langmuir isotherm was evaluate. In the literature, the wide variety  
 362 of cross linking agents and CDs, make difficult the comparison obtained results of adsorption.  
 363 Furthermore, to the best of the authors' knowledge, no adsorption studies of PMV from aqueous  
 364 media have been carried out so far. For this reason, we decided to present a table were compare  
 365 the results of polymers based on cyclodextrins, take into account that different organic  
 366 compounds, mainly pharmaceuticals, were employed in the related studies (Table 3 ).

367 **Table 3**  
 368 Comparison of the adsorption properties of different polymers based on cyclodextrins.

Pharmaceutical	Polymer	Adsorption capacity, $q_{\max}$ ( $\text{mg g}^{-1}$ )	References
Phenolphthalein	$\beta$ -CDs-GNS	468	(Tan and Hu, 2017)
Ciprofloxacin	$\beta$ -CD-EDTA	448	(Yu et al., 2018)
Ibuprofen	$\beta$ -CD-CH	240.7	(Bany-Aiesh et al., 2015)
Chloroxylenol	$\beta$ -CD-TFP	144.1	(Zhou et al., 2019)
Carbamazepine	$\beta$ -CD-TFP	136.4	(Zhou et al., 2019)
Bisphenol A	$\beta$ -CD-TFP	88.00	(Alsbaiee et al., 2016)

17 $\beta$ -estradiol	$\beta$ -CD-PLGA	85.80	(Jiang et al., 2017)
Aspirin	$\beta$ -CD-N-CNT	71.94	(Mphahlele et al., 2015)
Rhodamine B	$\beta$ -CD-DPC	56.88	(Lee et al., 2019)
Pimavanserin	$\beta$ -CD-CDI	52.08	This work
Procaine	CS-ED-CD	47.03	(Zhao et al., 2017)
Imipramine	CS-ED-CD	44.30	(Zhao et al., 2017)
Paracetamol	$\beta$ -CD-N-CNT	41.00	(Mphahlele et al., 2015)
Congo red	$\beta$ -CD-HMDI	36.2	(Ozmen and Yilmaz, 2007)
Direct Red 83:1	HP- $\alpha$ -CDs-EPI	23.4	(Pellicer et al., 2018)
Pimavanserin	$\beta$ -CD-CDI	23.26	This work
Direct Blue 78	$\gamma$ -CD-EPI	14.16	(Semeraro et al., 2018)
Phenol	$\beta$ -CD-CA	13.80	(Zhao et al., 2009)
Methyltestosterone	$\beta$ -CD-Si	13.09	(Carvalho et al., 2019)
Methylene Blue	$\beta$ -CD-M	11.43	(Yadav et al., 2019)
Direct Blue 78	$\beta$ -CD-EPI	4.99	(Semeraro et al., 2018)
p-Nitrophenol	$\beta$ -CD-HMDI	1.00	(Salgin et al., 2017)

369 GNS- graphene, EDTA- ethylenediaminetetraacetic acid, TFP -Tetrafluoroterephthalonitrile, N-CNT- nitrogen

370 doped carbon nanotubes, DPC- diphenyl carbonate, CDI- diimidazole carbonate, HMDI- hexamethylene

371 diisocyanate, EPI- epichlorohydrin, CA- citric acid, M- Maleic acid

### 372 3.3. Adsorption mechanism studies

373 Because the adsorption process by NS mainly consists in the inclusion, we decided to take  
374 a closer look on this phenomenon. We chose  $^1\text{H}$  NMR spectroscopy allowing obtaining the  
375 information about the stoichiometry and the structure of PMV supramolecular complexes  
376 formed with CDs.

### 377 3.3.1. Inclusion phenomena

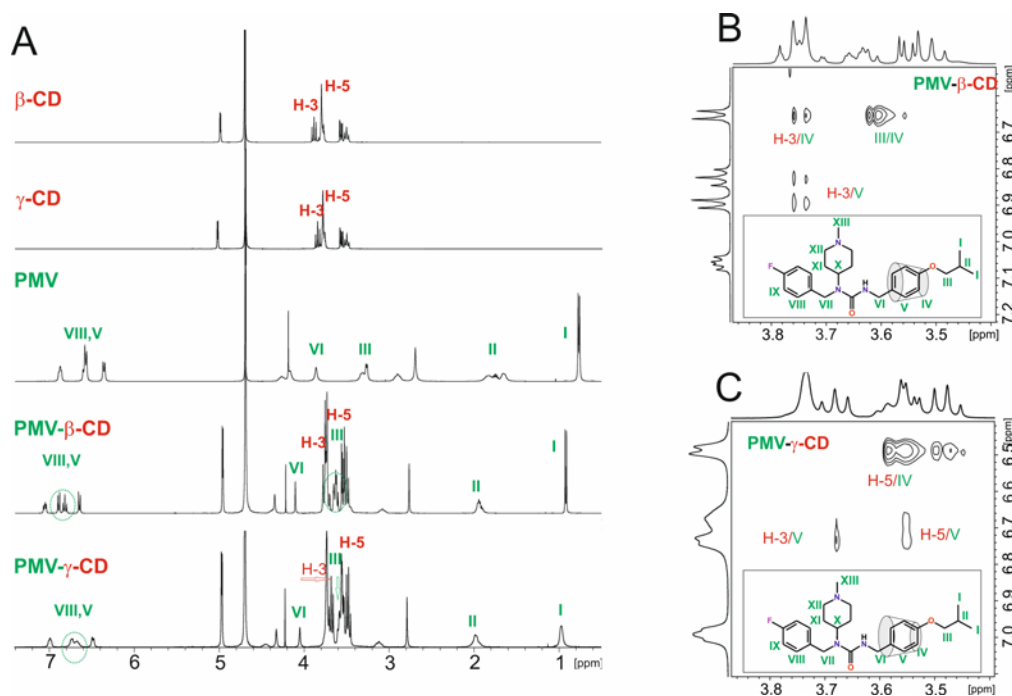
378 A characteristic feature of the signals present in the  $^1\text{H}$  NMR spectrum of PMV is the  
379 widening resulting from the presence of chiral centers. As a consequence, a mixture of  
380 enantiomers is analyzed instead of one. The PMV spectrum is significantly simplified when  
381 forming a complex with  $\beta$ -CD, which may indicate that only one of the isomers is included.  
382 The PMV molecule is too large to fit into the host cavity. At the same time, it consists of three  
383 important moieties: 4-fluorobenzylamine (**A**), 4-isobutylbenzylamine (**B**) and *N*-  
384 methylpiperidine (**C**), each of which can form inclusion complexes. Analyzing further the  
385 recorded spectra, typical changes in the chemical shifts of internal CD protons (H-3 and H-5)  
386 were observed, resulting from the involvement in inclusion complex formation. The spectra of  
387  $\beta$ -CD and  $\gamma$ -CD complexes are presented in Fig. 6A. Discussed CDs internal protons are down  
388 fielded. The chemical shifts ( $\Delta\delta$ ) of  $\beta$ -CD is -0.150 for H-3 and -0.127 for H-5. In the case of  
389  $\gamma$ -CD,  $\Delta\delta$  for the same protons are -0.168 and -0.179, respectively (Table S6).

390 In comparison to the free drug spectrum, the spectra of inclusion complexes with CDs  
391 show the most change in aromatic field. The **B** moiety protons do not overlap with aromatic  
392 protons of **A** moiety, but separate/particular peaks are observed. The **B** moiety of PMV probably  
393 is included in the CD cavity. Analyzed protons have a larger chemical shifts in PMV- $\beta$ -CD  
394 complex than protons of **A** moiety. In the case of the PMV- $\gamma$ -CD complex, separate/particular  
395 peaks broadened may indicate fast exchange, or be a result of the larger size of the  $\gamma$ -CD cavity,  
396 enabling the formation of complexes with various PMV stereoisomers.

397 The stoichiometry of PMV with  $\beta$ - and  $\gamma$ -CD inclusion complexes were determined by  
398 Jobs method. The plots of Fig. S11 show that for the both binary systems the maximum of the  
399 curves is obtained for  $r = 0.5$ , that indicates 1:1 host-guest stoichiometry.

400 Unfortunately,  $^1\text{H}$  NMR spectra give not an unambiguous response which of the two  
401 aromatic rings of PMV is involved in the complexation, the geometry of the complexes was

402 analyzed considering intermolecular NOEs obtained from ROESY spectra (Fig. 6B and 6C).  
 403 The obtained results show that PMV insert to  $\beta$ - and  $\gamma$ -CD cavity from the side of **B** moiety. As  
 404 visualized in Fig. 6B and 6C, PMV is inserted deeper in  $\gamma$ -CD hydrophobic cavity than in  $\beta$ -  
 405 CD, since the cross peaks between IV protons of **B** moiety of guest with internal H-3 protons  
 406 (from the side of wider rim) are not visible, but occur between H-5 protons (from the side of  
 407 narrow rim).

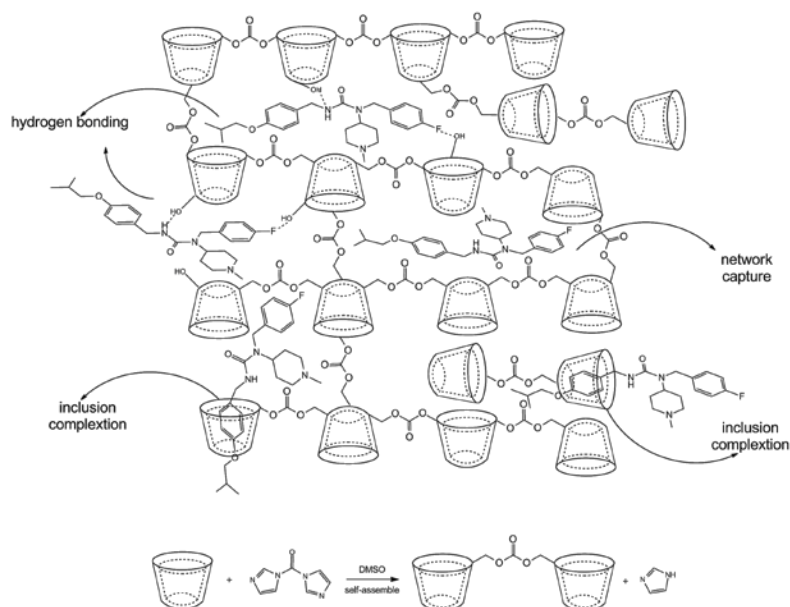


408  
 409 **Fig. 6.** <sup>1</sup>H NMR (A), and ROESY spectra for PMV with  $\beta$ - (B) and  $\gamma$ -CD (C).

### 410 3.3.2. Pore texture

411 The obtained materials consist of particles with a dimension of 172 nm and 431 nm for  
 412  $\beta$ -NS and  $\gamma$ -NS, respectively (SI, Fig. S5). The main structural elements of obtained sponges  
 413 are mesopores (Barrett-Joyner-Halenda method, Fig. S4, Table S5). The **B** moiety, which is  
 414 suspected for complex formation, is small in size, so it can be adsorbed in micropores. The  
 415 analysis of the NS surface showed that the micropores have only  $\beta$ -NS, they constitute 13% of  
 416 the total BET surface area (Harkins and Jura t-Plot, Fig. S3, Table S4).

417 Considering the obtained results, we believe that the mechanism of CD-NS sorption involves  
418 inclusion complexation, hydrogen bonding and physical sorption in the network (**Fig. 7.**).



420 **Fig. 7.** Cross-linked structure of  $\beta$ -CD-NS and related sorption mechanism of PMV.

421 Comparing the created structures with the use of two cyclodextrins, the basic differences are  
422 the size of the cavity and the packing of toruses in the network. It is well known that the presence  
423 of internal hydrogen bonds in  $\beta$ -CD is responsible for additional stiffening of the molecule.  
424 Perhaps, in this particular case, it is also the reason for creating additional appropriately  
425 dimensioned spaces between torus able to trap PMV. The situation is different with  $\gamma$ -CDs. The  
426 large rim allows easy guest entry and exit. The flexible structure does not allow the creation of  
427 neat spaces between the toruses. As a result, the material is seemingly the same and in fact quite  
428 different.

429

### 430 3.4. Adsorption study of PMV in real post-reaction raffinates

431 PMV is on the market only since 2016, which explains the lack of literature data on the  
432 presence of the drug in the environment. Our preliminary studies have clearly shown that PMV  
433 does not degrade during biological treatment and is toxic to aquatic organisms. According to

434 one of the principles of green chemistry, it is always better to prevent than eliminate undesirable  
435 effects, PMV synthesis requires total drug recovery from all produced streams. For this purpose,  
436 three drug syntheses were performed using the patent description US 2018/0208556 A1 (Chen-  
437 Wei and Chin-Wei, 2018), which seems to be the most ecofriendly among those described in  
438 the literature. It is one pot synthesis provided in biodegradable organic solvent – ethyl acetate.  
439 Waste streams are formed only during purification time, when postreaction mixture is washed  
440 with water. Of course, part of the drug dissolves in the aqueous phases, consequently  
441 contaminating the raffinate. Small scale synthesis produces approximately 24 mL of raffinate  
442 for each gram of crude PMV. One gram of PMV is also the amount that a single patient takes  
443 in just one month of treatment. Thus, in the final phase, three streams of raffinate samples  
444 containing from 190 to 210 mg L<sup>-1</sup> PMV were obtained (Table S1).

445 Literature data shows that during other PMV synthesis, not only aqueous, but also acidic and  
446 briny raffinates are also produced. Therefore, two mixtures containing comparable amounts of  
447 hydrochloric acid, sodium chloride and ammonium chloride to those used in additional patents  
448 have been prepared (Table S2). All raffinates were used in sorption tests by means of the best  
449 adsorbents, i.e.  $\beta$ -NS and activated carbon O-C303 (Table 4).

450 Comparing the results of sorption of PMV from aqueous raffinates, it can be stated that both  
451 adsorbents ensure the quantitative removal of the drug from salt-free aqueous solutions. In the  
452 case of low pH and presence of salt, the PMV uptake efficiency by activated carbon is reduced  
453 by 5%. Even more troublesome is to remove the drug from concentrated mixtures of sodium  
454 and ammonium chlorides. In this case, as much as 15% of the drug remains in the waste stream.  
455 Our material, regardless of the raffinate composition, selectively and quantitatively binds PMV.  
456 This is due to the specifics of the impacts. NS centers responsible for PMV inclusion are  
457 hydrophobic and remain indifferent to relatively small charged individuals molecules. It is also  
458 possible to recover adsorbed PMV during the regeneration of with methanol. The resulting



459 solutions contain only the drug and can be directed after concentration to the next stage of  
 460 production, in which the pimavanserin base is converted into the corresponding salt. At the  
 461 same time, the methanol separated during distillation can be reused for desorption of PMV from  
 462 NS. Desorption of API from activated carbon, carried out in an analogous manner, is  
 463 impossible, which means that each portion of activated carbon after the process becomes a  
 464 hazardous waste.

465

466 Table 4 Percentage removal efficiency of PMV adsorption on  $\beta$ -NS (75 mg) and AC-O-C303 (25 mg); contact  
 467 time = 30 min; room temperature, rotational speed (1,000 rpm).

Raffinate*	$C_0$ (mg L <sup>-1</sup> )	O-C303 removal efficiency of PMV (%)	$\beta$ -NS removal efficiency of PMV (%)	Recovery of adsorbed PMV from $\beta$ -NS (%)	Purity of desorbed PMV (HPLC method)
B-1	0.190			95	98
B-2	0.195	100	100	96	99
B-3	0.201			95	99
A		100	100	95	98
C-1	0.200	85	100	94	97
C-2		95	100	93	

468 \*Each result is an average of three PMV tests carried out in parallel. Raffinate descriptions are available in table  
 469 1 and 2 in ESI.

470

#### 471 4. Conclusions

472 The preliminary toxicity results of this work show that PMV can be classified as  
 473 hazardous ( $EC_{50} = 8 \text{ mgL}^{-1}$ ). In biological wastewater treatment plant, the degree of PMV  
 474 degradation is only 37% and can pose a serious environmental problem in the future. The  
 475 obtained NSs are suitable for quantitative removal of PMV from model waste waters as well as  
 476 from real post-reaction raffinates, even those characterized by the very low pH and high salt



477 concentration. Data obtained during adsorption experiments were expressed using the  
478 Langmuir and Freundlich isotherms. The  $\beta$ - and  $\gamma$ -NS presented a maximum adsorption  
479 capacity of 52.08 mg g<sup>-1</sup> and 23.26 mg g<sup>-1</sup> towards the PMV, respectively. Although, the results  
480 show that both isotherms are linear within all established initial concentrations, the adsorption  
481 process was better represented by Freundlich isotherm ( $R^2=0.99$  for  $\beta$ -NS and  $R^2=0.98$  for  $\gamma$ -  
482 NS). Despite of small specific surface area of obtained NSs, the effectiveness of adsorption of  
483 PMV from aqueous media were similar to active carbons and adsorption process took place in  
484 impressively short time (60 s). The obtained NSs materials are fully and easily regenerable  
485 without affecting their structure. The inclusion phenomena are extremely specific and allow for  
486 a much better use of the adsorbent's specific surface area. The mechanism of sorption is  
487 complex, dominated by chemisorptions via the formation of an inclusion complex with  
488 cyclodextrin present in the NSs structure, and to a lesser extent by surface adsorption and  
489 diffusion into the polymer network. However, diffusion into the polymer network is also  
490 important. The 4-isobutyl-benzylamine group is responsible for complex formation and this  
491 group is small in size, so it can be also adsorbed in micropores. Such pore size is presented only  
492 in  $\beta$ -NS material, and is also responsible for somewhat better results of PMV adsorption  
493 efficiency compared to  $\gamma$ -NS.

494 The experimental results clearly show that NS in the area of adsorbents are promising  
495 and can be successfully used to separate organic pollutants from industrial raffinates and  
496 wastewater.

497

#### 498 **Conflicts of interest**

499 There are no conflicts to declare.

500

#### 501 **Acknowledgements**

502 The authors are grateful for financial support provided by Gdańsk University of  
503 Technology, DS 033150.

504

505

## 506 **References**

507 Al-Asheh, S., Banat, F., Abu-Aitah, L., 2003. Adsorption of phenol using different types of  
508 activated bentonites. *Sep. Purif. Technol.* 33, 1–10. [https://doi.org/10.1016/S1383-](https://doi.org/10.1016/S1383-5866(02)00180-6)  
509 [5866\(02\)00180-6](https://doi.org/10.1016/S1383-5866(02)00180-6)

510 Alsaiee, A., Smith, B.J., Xiao, L., Ling, Y., Helbling, D.E., Dichtel, W.R., 2016. Rapid  
511 removal of organic micropollutants from water by a porous  $\beta$ -cyclodextrin polymer.  
512 *Nature* 529, 190–194. <https://doi.org/10.1038/nature16185>

513 American Public Health Association (APHA), 2005. *Standard Methods for the Examination*  
514 *of Water and Wastewater*, 21st ed, American Public Health Association. American  
515 Public Health Association, Washington.

516 Arora, P., Dhingra, N., 2018. Cyclodextrin. A Versatile Ingredient. InTechOpen.  
517 <https://doi.org/10.5772/intechopen.69187>

518 Bany-Aiesh, H., Banat, R., Al-Sou'od, K., 2015. Kinetics and adsorption isotherm of  
519 ibuprofen onto grafted  $\beta$ -CD/chitosan polymer. *Am. J. Appl. Sci.* 12, 917–930.  
520 <https://doi.org/10.3844/ajassp.2015.917.930>

521 Barrett, E.P., Joyner, L.G., Halenda, P.P., 1951. The Determination of Pore Volume and Area  
522 Distributions in Porous Substances. I. Computations from Nitrogen Isotherms. *J. Am.*  
523 *Chem. Soc.* 73, 373–380. <https://doi.org/10.1021/ja01145a126>

524 Bo, L., Gao, N., Liu, J., Gao, B., 2016. The competitive adsorption of pharmaceuticals on  
525 granular activated carbon in secondary effluent. *Desalin. Water Treat.* 57, 17023–17029.  
526 <https://doi.org/10.1080/19443994.2015.1082942>



- 527 Brunauer, S., Emmett, P.H., Teller, E., 1938. Adsorption of Gases in Multimolecular Layers.  
528 J. Am. Chem. Soc. 60, 309–319. <https://doi.org/10.1021/ja01269a023>
- 529 Carvalho, L.B., Chagas, P.M.B., Marques, T.R., Razafitianamaharavo, A., Pelletier, M.,  
530 Nolis, P., Jaime, C., Thomasi, S.S., Pinto, L.D.M.A., 2019. Removal of the synthetic  
531 hormone methyltestosterone from aqueous solution using a  $\beta$ -cyclodextrin/silica  
532 composite. J. Environ. Chem. Eng. 7. <https://doi.org/10.1016/j.jece.2019.103492>
- 533 Chen-Wei, H., Chin-Wei, T., 2018. Method for preparing Pimavanserin. US 2018/0208556  
534 A1.
- 535 Chendo, I., Ferreira, J.J., 2016. Pimavanserin for the treatment of Parkinson's disease  
536 psychosis. Expert Opin. Pharmacother. 17, 2115–2124.  
537 <https://doi.org/10.1080/14656566.2016.1234609>
- 538 Combs, B.L., Cox, A.G., 2017. Update on the treatment of Parkinson's disease psychosis:  
539 Role of pimavanserin. Neuropsychiatr. Dis. Treat. 13, 737–744.  
540 <https://doi.org/10.2147/NDT.S108948>
- 541 Corsi, I., Fiorati, A., Grassi, G., Bartolozzi, I., Daddi, T., Melone, L., Punta, C., 2018.  
542 Environmentally sustainable and ecosafe polysaccharide-based materials for water nano-  
543 treatment: An eco-design study. Materials (Basel). 11, 1–23.  
544 <https://doi.org/10.3390/ma11071228>
- 545 Crini, G., Bertini, S., Torri, G., Naggi, A., Sforzini, D., Vecchi, C., Janus, L., Lekchiri, Y.,  
546 Morcellet, M., 1998. Sorption of Aromatic Compounds in Water Using Insoluble  
547 Cyclodextrin Polymers. J Appl Polym Sci 68, 1973–1978.  
548 [https://doi.org/10.1002/\(SICI\)1097-4628\(19980620\)68:12<1973::AID-  
549 APP11>3.0.CO;2-T](https://doi.org/10.1002/(SICI)1097-4628(19980620)68:12<1973::AID-APP11>3.0.CO;2-T)
- 550 Ensano, B.M.B., Borea, L., Naddeo, V., Belgiorno, V., G, D.L.M.D., Jr, F.C., 2017. Removal  
551 of pharmaceutical compounds by electrochemical processes in real wastewater. Remov.



552 Pharm. Compd. by Electrochem. Process. real wastewater 2015–2018.

553 Fourmentin, S., Crini, G., Lichtfouse, E., 2018. Cyclodextrin Applications in Medicine, Food,  
554 Environment and Liquid Crystals, 1st ed. Springer International Publishing.  
555 <https://doi.org/10.1007/978-3-319-76162-6>

556 Gant, T., Sarshar, S., 2008. Deuterated Pimavanserin 1-(4-fluorobenzyl)-3-(4-  
557 isobutoxybenzyl)-1-(L-methyl-piperidin-4-yl)-urea. WO 2008/141057 A1.

558 Hall, K.R., Eagleton, L.C., Acrivos, A., Vermeulen, T., 1966. Pore- and solid-diffusion  
559 kinetics in fixed-bed adsorption under constant-pattern conditions. Ind. Eng. Chem.  
560 Fundam. 5, 212–223. <https://doi.org/10.1021/i160018a011>

561 Ho, Y.S., Porter, J.F., McKay, G., 2002. Equilibrium isotherm studies for the sorption of  
562 divalent metal ions onto peat: copper, nickel, and lead single component systems. Water,  
563 Air, Soil Pollut. 141, 1–33.

564 Janarthanan, P., Veeramachineni, A.K., Loh, X.J., 2016. Biodegradable Polysaccharides. Ref.  
565 Modul. Mater. Sci. Mater. Eng. 1–12. [https://doi.org/10.1016/B978-0-12-803581-  
566 8.09218-3](https://doi.org/10.1016/B978-0-12-803581-8.09218-3)

567 Jiang, L., Liu, Y., Liu, Shaobo, Hu, Xinjiang, Zeng, G., Hu, Xi, Liu, Simian, Liu, Shaoheng,  
568 Huang, B., Li, M., 2017. Fabrication of  $\beta$ -cyclodextrin/poly (L-glutamic acid) supported  
569 magnetic graphene oxide and its adsorption behavior for 17 $\beta$ -estradiol. Chem. Eng. J.  
570 308, 597–605. <https://doi.org/10.1016/j.cej.2016.09.067>

571 Kanakaraju, D., Glass, B.D., Oelgemöller, M., 2018. Advanced oxidation process-mediated  
572 removal of pharmaceuticals from water: A review. J. Environ. Manage. 219, 189–207.  
573 <https://doi.org/10.1016/j.jenvman.2018.04.103>

574 Karoyo, A.H., Wilson, L.D., 2016. Preparation and Characterization of a Polymer-Based  
575 “Molecular Accordion.” Langmuir 32, 3066–3078.  
576 <https://doi.org/10.1021/acs.langmuir.6b00099>



- 577 Kovalova, L., Knappe, D.R.U., Lehnberg, K., Kazner, C., Hollender, J., 2013. Removal of  
578 highly polar micropollutants from wastewater by powdered activated carbon. *Environ.*  
579 *Sci. Pollut. Res.* 20, 3607–3615. <https://doi.org/10.1007/s11356-012-1432-9>
- 580 Lee, Y.S., Lim, Y.T., Choi, W.S., 2019. One-step synthesis of environmentally friendly  
581 superhydrophilic and superhydrophobic sponges for oil/water separation. *Materials*  
582 (Basel). 12. <https://doi.org/10.3390/ma12071182>
- 583 Mamba, B.B., Krause, R.W., Malefetse, T.J., Nxumalo, E.N., 2007. Monofunctionalized  
584 cyclodextrin polymers for the removal of organic pollutants from water. *Environ. Chem.*  
585 *Lett.* 5, 79–84. <https://doi.org/10.1007/s10311-006-0082-x>
- 586 McKay, G., 2007. Adsorption of dyestuffs from aqueous solutions with activated carbon I:  
587 Equilibrium and batch contact-time studies. *J. Chem. Technol. Biotechnol.* 32, 759–772.  
588 <https://doi.org/10.1002/jctb.5030320712>
- 589 Menapace, H.M., Diaz, N., Weiss, S., 2008. Electrochemical treatment of pharmaceutical  
590 wastewater by combining anodic oxidation with ozonation. *J. Environ. Sci. Heal. - Part*  
591 *A Toxic/Hazardous Subst. Environ. Eng.* 43, 961–968.  
592 <https://doi.org/10.1080/10934520801974558>
- 593 Morin-Crini, N., Crini, G., 2013. Environmental applications of water-insoluble  $\beta$ -  
594 cyclodextrin- epichlorohydrin polymers. *Prog. Polym. Sci.* 38, 344–368.  
595 <https://doi.org/10.1016/j.progpolymsci.2012.06.005>
- 596 Morin-Crini, N., Winterton, P., Fourmentin, S., Wilson, L.D., Fenyvesi, É., Crini, G., 2018.  
597 Water-insoluble  $\beta$ -cyclodextrin–epichlorohydrin polymers for removal of pollutants from  
598 aqueous solutions by sorption processes using batch studies: A review of inclusion  
599 mechanisms. *Prog. Polym. Sci.* 78, 1–23.  
600 <https://doi.org/10.1016/j.progpolymsci.2017.07.004>
- 601 Mphahlele, K., Onyango, M.S., Mhlanga, S.D., 2015. Adsorption of aspirin and paracetamol



602 from aqueous solution using Fe/N-CNT/ $\beta$ -cyclodextrin nanocomposites synthesized via  
603 a benign microwave assisted method. *J. Environ. Chem. Eng.* 3, 2619–2630.  
604 <https://doi.org/10.1016/j.jece.2015.02.018>

605 Orprecio, R., Evans, C.H., 2003. Polymer-Immobilized Cyclodextrin Trapping of Model  
606 Organic Pollutants in Flowing Water Streams. *J. Appl. Polym. Sci.* 90, 2103–2110.  
607 <https://doi.org/10.1002/app.12818>

608 Ozmen, E.Y., Yilmaz, M., 2007. Use of  $\beta$ -cyclodextrin and starch based polymers for sorption  
609 of Congo red from aqueous solutions. *J. Hazard. Mater.* 148, 303–310.  
610 <https://doi.org/10.1016/j.jhazmat.2007.02.042>

611 Pellicer, J.A., Rodríguez-López, M.I., Fortea, M.I., Gabaldón Hernández, J.A., Lucas-  
612 Abellán, C., Mercader-Ros, M.T., Serrano-Martínez, A., Núñez-Delicado, E., Cosma, P.,  
613 Fini, P., Franco, E., García, R., Ferrándiz, Marcela, Pérez, E., Ferrándiz, Miguel, 2018.  
614 Removing of Direct Red 83:1 using  $\alpha$ - and HP- $\alpha$ -CDs polymerized with epichlorohydrin:  
615 Kinetic and equilibrium studies. *Dye. Pigment.* 149, 736–746.  
616 <https://doi.org/10.1016/j.dyepig.2017.11.032>

617 Pratt, D.Y., Wilson, L.D., Kozinski, J.A., Mohart, A.M., 2010. Preparation and Sorption  
618 Studies of  $\beta$ -Cyclodextrin/ Epichlorohydrin Copolymers. *J. Appl. Polym. Sci.* 116,  
619 2982–2989. <https://doi.org/10.1002/app>

620 Putra, E.K., Pranowo, R., Sunarso, J., Indraswati, N., Ismadji, S., 2009. Performance of  
621 activated carbon and bentonite for adsorption of amoxicillin from wastewater:  
622 Mechanisms, isotherms and kinetics. *Water Res.* 43, 2419–2430.  
623 <https://doi.org/10.1016/j.watres.2009.02.039>

624 Rao, D.G., Senthilkumar, R., Byrne, J.A., Feroz, S., 2012. Wastewater Treatment: Advanced  
625 Processes and Technologies. CRC Press.

626 Rapolu, R.K., Prasada Raju, V.V.N.K.V., Chavali, M., Mulakayala, N., 2019. Novel and



- 627 Environmentally Friendly Synthesis of Pimavanserin (5-HT<sub>2A</sub> Receptor). *Asian J.*  
628 *Chem.* 31, 723–726. <https://doi.org/10.14233/ajchem.2019.21808>
- 629 Salgın, S., Salgın, U., Vatansever, Ö., 2017. Synthesis and Characterization of  $\beta$ -Cyclodextrin  
630 Nanosponge and Its Application for the Removal of p- Nitrophenol from Water.  
631 *WILEY-VCH* 45, 1–20. <https://doi.org/10.1002/acr>.
- 632 San Miguel, G., Lambert, S.D., Graham, N.J.D., 2001. The regeneration of field-spent  
633 granular-activated carbons. *Water Res.* 35, 2740–2748. [https://doi.org/10.1016/S0043-](https://doi.org/10.1016/S0043-1354(00)00549-2)  
634 [1354\(00\)00549-2](https://doi.org/10.1016/S0043-1354(00)00549-2)
- 635 Semeraro, P., Gabaldón, J.A., Fini, P., Núñez, E., Pellicer, J.A., Rizzi, V., Cosma, P., 2018.  
636 Removal of an Azo Textile Dye from Wastewater by Cyclodextrin-Epichlorohydrin  
637 Polymers. *Cyclodext. - A Versatile Ingred.* <https://doi.org/10.5772/intechopen.72502>
- 638 Shojaee Nasirabadi, P., Saljoughi, E., Mousavi, S.M., 2016. Membrane processes used for  
639 removal of pharmaceuticals, hormones, endocrine disruptors and their metabolites from  
640 wastewaters: A review. *Desalin. Water Treat.* 57, 24146–24175.  
641 <https://doi.org/10.1080/19443994.2016.1140081>
- 642 Szejtli, V.J., Fenyvesi, E., Zsádon, B., 1978. Cyclodextrinpolymere. *Starch-Starke* 127, 6–7.
- 643 Tan, P., Hu, Y., 2017. Improved synthesis of graphene/ $\beta$ -cyclodextrin composite for highly  
644 efficient dye adsorption and removal. *J. Mol. Liq.* 242, 181–189.  
645 <https://doi.org/10.1016/j.molliq.2017.07.010>
- 646 Trotta, F., Tumiatti, W., 2005. Cross-linked polymers based on cyclodextrins for removing  
647 polluting agents. *US* 2005/0154198A1.
- 648 Walter, S., Mitkidis, K., 2018. The Risk Assessment of Pharmaceuticals in the Environment:  
649 EU and US Regulatory Approach. *Eur. J. Risk Regul.* 39, 1–21.  
650 <https://doi.org/10.1017/err.2018.33>
- 651 Weltens, R., Deprez, K., Michiels, L., 2014. Validation of Microtox as a first screening tool



652 for waste classification. *Waste Manag.* 34, 2427–2433.  
653 <https://doi.org/10.1016/j.wasman.2014.08.001>

654 Yadav, M., Das, M., Savani, C., Thakore, S., Jadeja, R., 2019. Maleic Anhydride Cross-  
655 Linked  $\beta$ -Cyclodextrin-Conjugated Magnetic Nanoadsorbent: An Ecofriendly Approach  
656 for Simultaneous Adsorption of Hydrophilic and Hydrophobic Dyes. *ACS Omega* 4,  
657 11993–12003. <https://doi.org/10.1021/acsomega.9b00881>

658 Yilmaz, E., Memon, S., Yilmaz, M., 2010. Removal of direct azo dyes and aromatic amines  
659 from aqueous solutions using two  $\beta$ -cyclodextrin-based polymers. *J. Hazard. Mater.* 174,  
660 592–597. <https://doi.org/10.1016/j.jhazmat.2009.09.093>

661 Yu, F., Chen, D., Ma, J., 2018. Adsorptive removal of ciprofloxacin by ethylene  
662 diaminetetraacetic acid/ $\beta$ -cyclodextrin composite from aqueous solution. *New J. Chem.*  
663 42, 2216–2223. <https://doi.org/10.1039/c7nj03770h>

664 Zhao, D., Zhao, L., Zhu, C.S., Huang, W.Q., Hu, J.L., 2009. Water-insoluble  $\beta$ -cyclodextrin  
665 polymer crosslinked by citric acid: Synthesis and adsorption properties toward phenol  
666 and methylene blue. *J. Incl. Phenom. Macrocycl. Chem.* 63, 195–201.  
667 <https://doi.org/10.1007/s10847-008-9507-4>

668 Zhao, F., Repo, E., Yin, D., Chen, L., Kalliola, S., Tang, J., Iakovleva, E., Tam, K.C.,  
669 Sillanpää, M., 2017. One-pot synthesis of trifunctional chitosan-EDTA- $\beta$ -cyclodextrin  
670 polymer for simultaneous removal of metals and organic micropollutants /. *Sci. Rep.* 7,  
671 1–14. <https://doi.org/10.1038/s41598-017-16222-7>

672 Zhou, Y., Cheng, G., Chen, K., Lu, J., Lei, J., Pu, S., 2019. Adsorptive removal of bisphenol  
673 A, chloroxylenol, and carbamazepine from water using a novel  $\beta$ -cyclodextrin polymer.  
674 *Ecotoxicol. Environ. Saf.* 170, 278–285. <https://doi.org/10.1016/j.ecoenv.2018.11.117>

675 Zupanc, M., Kosjek, T., Petkovšek, M., Dular, M., Kompare, B., Širok, B., Blažeka, Ž.,  
676 Heath, E., 2013. Removal of pharmaceuticals from wastewater by biological processes,





677 hydrodynamic cavitation and UV treatment. *Ultrason. Sonochem.* 20, 1104–1112.

678 <https://doi.org/10.1016/j.ultsonch.2012.12.003>

679

680

681

682

683

684

685

686

687

688

689